

In vitro and in vivo effects of an anti-mouse endoglin (CD105)–immunotoxin on the early stages of mouse B16MEL4A5 melanoma tumours

Raquel Muñoz · Yolanda Arias · José Miguel Ferreras · Pilar Jiménez · Carmen Langa · María Angeles Rojo · Manuel José Gayoso · Damián Córdoba-Díaz · Carmelo Bernabéu · Tomás Girbés

Received: 11 May 2012 / Accepted: 25 September 2012 / Published online: 18 October 2012
© Springer-Verlag Berlin Heidelberg 2012

Abstract TGF-beta superfamily co-receptors are emerging as targets for cancer therapy, acting both directly on cells and indirectly on the tumour neovasculature. Endoglin (CD105), an accessory component of the TGF-beta receptor complex, is expressed in certain melanoma cell lines and the endothelial cells of tumour neovessels. Targeting endoglin with immunotoxins is an attractive approach for actively suppressing the blood supply to tumours. Here, we report evidence indicating that endoglin is expressed in mouse melanoma B16MEL4A5 and mouse

fibroblast L929 cell lines. We prepared an immunotoxin to target endoglin by coupling the rat anti-mouse MJ7/18 (IgG2a) monoclonal antibody (mAb) to the non-toxic type 2 ribosome-inactivating protein nigrin b (Ngb) with N-succinimidyl 3-(2-pyridyldithio)-propionate (SPDP) as a linker with a molar nigrin b at a MJ7/18 stoichiometry of 2:1. The MJ7-Ngb immunotoxin generated killed both cell lines, with IC_{50} values of 4.2×10^{-9} M for B16MEL4A5 and 7.7×10^{-11} M for L929 cells. For in vivo assays of the immunotoxin, B16MEL4A5 cells were injected subcutaneously into the right flanks of 6-week-old C57BL/6 J mice. When the animals developed palpable solid tumours, they were subjected to treatment with the immunotoxin. While treatment with either MJ7/18 mAb or Ngb did not affect tumour development, treatment with the immunotoxin completely and steadily blocked tumour growth up to 7 days, after which some tumours re-grew. Thus, vascular-targeting therapy with this anti-vascular immunotoxin could promote the destruction of newly created tumour vessels at early stages of B16MEL4A5 tumour development and readily accessible CD105+ B16MEL4A5 melanoma cells.

R. Muñoz · Y. Arias · J. M. Ferreras
Facultad de Ciencias, Departamento de Bioquímica y Biología Molecular, Universidad de Valladolid, 47005 Valladolid, Spain

P. Jiménez · T. Girbés (✉)
Nutrición y Bromatología-Facultad de Medicina y Centro de Investigación en Nutrición, Alimentación y Dietética (CINAD), Universidad de Valladolid, 47005 Valladolid, Spain
e-mail: girbes@bio.uva.es

C. Langa · C. Bernabéu
Centro de Investigaciones Biológicas, Consejo Superior de Investigaciones Científicas (CSIC) and Centro de Investigación Biomédica en Red de Enfermedades Raras (CIBERER), 28040 Madrid, Spain

M. A. Rojo
Escuela Politécnica, Universidad Europea Miguel de Cervantes, 47012 Valladolid, Spain

M. J. Gayoso
Facultad de Medicina, Departamento de Biología Celular, Histología y Farmacología, Universidad de Valladolid, 47005 Valladolid, Spain

D. Córdoba-Díaz
Facultad de Farmacia, Departamento de Farmacia y Tecnología Farmacéutica, Universidad Complutense de Madrid, 28040 Madrid, Spain

Keywords Melanoma · Nigrin b · Endoglin · Anti-endoglin antibody · Anti-tumour therapy

Introduction

It is well known that tumour masses as small as 1–2 mm³ require the formation of a new network of vessels to sustain blood flow [1]. The tumour core exerts a positive pressure that hinders the accumulation of anti-cancer drugs, thus leading to poorly effective therapies [2]. One of the current approaches to cancer therapy is based on the attack of the

new blood vessels, each supporting thousands of cancer cells in the tumour mass, rather than direct attack of cancer cells [3]. A direct consequence would be a reduction in the concentration of the anti-cancer drug required for therapy and therefore its harmful secondary or collateral effects.

One of the therapies used to target tumour neovasculature uses inhibitors of angiogenesis and is aimed at inhibiting the formation of new capillary vessels without interfering with pre-existing ones. Anti-angiogenic therapy seems to circumvent the problem of drug-acquired resistance [4, 5]. Nevertheless, tumours may still become resistant to anti-angiogenic therapy [6]. Tumour therapy with angiogenesis inhibitors is a rather slow process, but preclinical evidence indicates that combining these agents with conventional cytotoxic agents or radiation therapy results in additive or even synergistic anti-tumour effects [7]. Another approach to tumour therapy is vascular targeting with immunotoxins and radioantibodies as markers of the tumour neovasculature [8–10]. Thus, the destruction of the neovasculature using therapy with immunotoxins and radioantibodies is much faster than therapy with standard inhibitors of angiogenesis, leading to an efficient destruction of large tumour masses. Recently, Roodink and Leenders [1] have highlighted the need to complement the inhibition of neovasculature with other vascular-targeting therapy to avoid tumour progression in an angiogenesis-independent manner. Leukaemia and lung cancer regression promoted by anti-angiogenic therapy are favoured by vascular disruption of established tumour-supporting vessels [11, 12]. Furthermore, selective destruction of tumour neovasculature improves the delivery of chemotherapy to tumours [13]. Such an approach is much more aggressive than the sole inhibition of vessel growth and could have drawbacks associated with potential renal complications derived from the tumour necrosis [14].

One marker of tumour neovasculature is the TGF- β receptor endoglin (CD105) expressed in several mammalian tissues, especially those related to the proliferation of new vasculature [15–17]. Of particular interest is the fact that endoglin is overexpressed by up-regulation in the endothelial cells of the tumour neovasculature [18–20]. Endoglin is also present in some cancer cells, such as some melanoma [21, 22] and chorion carcinoma cells [23]. In breast carcinoma, vascular density, determined using anti-CD105 antibody, is correlated with tumour prognosis [24]. The risk of developing metastatic disease in colorectal cancer is related to the endoglin-positive vessel count [25]. Endoglin-assessed micro-vessel density is also associated with the recurrence of malignancy in laryngeal squamous cell carcinoma [26]. A further involvement of endoglin in cancer is that the plasma levels of soluble endoglin are correlated with metastasis in patients with breast cancer [19, 27]. Owing to the increased expression of endoglin in

tumour neovasculature, its targeting has been used for therapeutic purposes [20, 28–30], either as experimental anti-angiogenic radioimmunotherapy with ^{125}I -labelled antibodies cross-reacting with shared epitopes present in human and murine endoglin or as immunotoxin therapy using immunotoxins made of the same cross-reacting anti-endoglin antibodies and either the A chain of the ribosome-inactivating protein ricin or the deglycosylated A chain of ricin [30]. To date, ricin has been one of the ribosome-inactivating proteins most used in the construction of immunotoxins [31, 32]. Since the compound displays very high non-specific activity in mammalian cells and animals, isolated ricin A chain, deglycosylated ricin A chain and ricin blocked by chemical means to reduce non-specific toxicity have been used [33]. Another major problem with ricin is the promotion of vascular leak syndrome (VLS), which clearly limits the usefulness of ricin-containing immunotoxins [34].

Melanoma is one of the most aggressive tumours and an example of tumours containing phenotypically and genetically different cells. Such tumours display notable resistance to chemotherapy drugs, and they frequently relapse after initial remission [35]. Recently, it has been reported that the eradication of a minor subset of cells accounting for approximately 2 % of the tumour cells that co-express the high-molecular-weight melanoma-associated antigen (HMW-MAA) and CD20 eradicated melanoma tumour lesions [36, 37]. In the present work, we report the effects of an immunotoxin, MJ7-Ngb, containing an anti-CD105 antibody linked to the non-toxic type 2 ribosome-inactivating protein Ngb isolated from elderberry bark [38], on cultured mouse B16MEL4A5 melanoma cells. As a proof of concept, we studied its short-term effects on B16MEL4A5 melanoma tumours developed in C57BL/6 J mice. Our data indicate that the short-time destruction of melanoma neovasculature with the MJ7-Ngb immunotoxin eradicated the tumour mass.

Materials and methods

Chemical and biological materials

The sources of most of the chemicals and biochemicals used in this work were the same as reported previously [39]. N-succinimidyl 3-(2-pyridyldithio)-propionate (SPDP) was purchased from Sigma Chemical Co (St Louis, MO, USA). The CPD StartTM reagent used as the chemiluminescent substrate for alkaline phosphatase and the WST-1 [2-(4-iodophenyl)-3-(4-nitrophenyl)-5-(2,4-disulfophenyl)-2H-tetrazolium] tetrazolium salt were purchased from Boehringer Mannheim GmbH (Mannheim, Germany). Highly purified preparations of Ngb were obtained as

reported elsewhere [40]. The rat anti-mouse CD105 mAb (clone MJ7/18) was a kind gift from Dr. E. Butcher (Stanford University, Palo Alto, CA, USA). The secondary antibody coupled to alkaline phosphatase was obtained from Sigma. The B16MEL4A5 mouse melanoma cell line was obtained from the European Collection of Cell Cultures (ECACC) and was cultured in Dulbecco's modified Eagle's medium (DMEM) containing 10 % foetal calf serum (FCS). L929 mouse fibroblasts were grown in RPMI 1640 supplemented with 10 % FCS.

Flow cytometry

Immunofluorescence flow cytometry was carried out as described [41]. Briefly, cells were incubated with the primary rat mAbs anti-mouse CD105 (clone MJ7/18), anti-mouse CD3 (clone Y-19), anti-mouse MHC class I (clone P2G9) (generous gift from Dr. José M. Rojo, Centro de Investigaciones Biológicas, CSIC, Madrid) and anti-mouse CD49e (integrin alpha 5 chain; clone 5H10-27, Pharmingen) for 30 min at 4 °C. After two washes with PBS, cells were incubated with Alexa Fluor[®] 488 goat anti-rat IgG (Invitrogen) at 4 °C for 30 min. Finally, cells were washed twice with PBS, and their fluorescence was estimated with a FACSCalibur flow cytometer (BD Biosciences, Franklin Lakes, NJ, USA), using the logarithmic amplifiers. The percentage of positive cells, mean fluorescence intensity (FI) and forward light scatter were measured. Expression indexes (EI) were the result of positive cell percentages multiplied by the mean FI of the total cell population.

Preparation and analysis of the MJ7-Ngb immunotoxin

The conjugation of MJ7/18 mAb and Ngb was carried out upon their previous activation. For activation, 7.5 mg MJ7/18 mouse monoclonal antibody was dissolved to a concentration of 1.6 mg/mL in 50 mM Na-borate (pH 9) and incubated for 1 h at 30 °C with a fivefold molar excess of N-succinimidyl-3-(2-pyridylthio)-propionate. Then, the solution was dialysed overnight at 4 °C against 4 L of solution containing 140 mM NaCl and 5 mM sodium phosphate (pH 7.5). Also, 26 mg of Ngb was activated in a final volume of 2.25 mL with a molar equivalent of N-succinimidyl 3-(2-pyridylthio)-propionate exactly in the same way as with the MJ7/18 mAb. The activated Ngb was dialysed overnight, like the activated MJ7/18 mAb. Activated MJ7/18 monoclonal antibody was reduced with 50 mM dithiothreitol for 30 min at room temperature and subjected to chromatography in Sephadex G-25, equilibrated and eluted with a solution containing 140 mM NaCl and 5 mM sodium phosphate (pH 7.5) to remove unreacted SPDP and dithiothreitol. Then, the void volume containing

the activated MJ7/18 mAb was collected on the activated and dialysed Ngb. The conjugation reaction was carried out for 18 h with gentle stirring at room temperature. The solution was concentrated up to 6 mL with Amicon YM10 and further chromatographed through a Superdex 200 HiLoad 26/60 column equilibrated with 140 mM NaCl and 5 mM sodium phosphate (pH 7.5). Elution was carried out with the same buffer solution at 2 mL/min, collecting fractions of 5 mL. Fractions containing the immunotoxin were collected, pooled and further concentrated with Amicon YM10 up to 5 mL and stored as aliquots at –80 °C. The yield of a standard preparation was 5.7 mg of MJ7-Ngb. The analysis of proteins by SDS-gel electrophoresis was carried out in 5 % polyacrylamide gels in the absence of 2-mercaptoethanol (2-ME) or in 15 % polyacrylamide gels in the presence of 2-mercaptoethanol to promote the reduction of disulphide bonds and to release the different proteins forming the immunotoxin, as described elsewhere [39].

Cytotoxicity of MJ7-Ngb immunotoxin

The cytotoxic activity of the immunotoxin against B16MEL4A5 and L929 cell lines was assessed using a cell viability assay, as reported [39, 40]. Briefly, 3×10^3 cells, growing in 96-well plates, were incubated in 100 μ L of complete culture medium alone or with the corresponding amount of Ngb, unconjugated MJ7 mAb or MJ7-Ngb immunotoxin for 3 h at 37 °C under 5 % CO₂ to allow protein internalization. Then, the wells were washed, and the cells were incubated with fresh complete medium for 3 days. At the end of the incubation period, viability was assessed with the cell proliferation reagent WST-1 as reported previously [38].

SDS-polyacrylamide gel electrophoresis and immunoblotting

For immunoblotting studies, 1×10^6 B16MEL4A5 or L929 cells were lysed in 300 μ L of 100 mM Na₂HPO₄, 1 mM EDTA, 1 % (v/v) Triton X-100, pH 7.4, plus protease inhibitors 1 mM PMSF and 2 μ g/mL aprotinin for 20 min on ice. Insoluble material was removed by centrifugation at 6,500 rpm for 7 min at 4 °C. The proteins present in the supernatant were separated by SDS-PAGE in 7.5 % polyacrylamide gels in the absence of 2-ME. After electrophoresis, the resolved proteins were electro-transferred onto a PVDF membrane. After blocking, blots were incubated first with anti-endoglin (clone MJ7/18) or anti- β -actin (clone AC-15, Sigma) mAbs and then with alkaline phosphatase-linked secondary antibody. The blots were then washed and probed with CPD-Star[™] in alkaline buffer.

In vivo treatments

For the in vivo studies, 6-week-old male C57BL/6 J mice (Harlan laboratories, Barcelona, Spain) were used. They were supplied with food and water *ab libitum*. For melanoma transplantation experiments, cultured B16MEL4A5 cells were washed twice using HBSS (Hank's balanced salt solution) and then re-suspended in the same buffer. A volume of 50 μL containing 1.25×10^5 cells was inoculated subcutaneously (s.c.) into the right flanks of the mice to establish subcutaneous tumours. Treatment was initiated between 1 and 2 weeks after cell inoculation when the tumour was palpable. The immunotoxin MJ7-Ngb was administered intravenously at a dose of 0.625 mg/kg body weight in 100 μL PBS containing 0.1 % mouse serum albumin and 0.1 M lactose via the tail vein. The treatment was repeated 12 and 24 h after the first injection. The Ngb and the MJ7/18 mAb were also injected in three doses equivalent to the amount of toxin and antibody conjugated in the immunotoxin, 0.271 mg/kg body weight and 0.354 mg/kg body weight, respectively. The control group of mice was injected with 100 μL PBS containing 0.1 % mouse serum albumin and 0.1 M lactose via the tail vein. The size of the tumours was measured daily with a calliper.

Histological analysis

All animals were anaesthetized and perfused transcardially with 4 % paraformaldehyde in phosphate buffer. Tumours were removed, washed, post-fixed in fixative for 24 h and paraffin wax-embedded for light microscopy studies. Histological sections of the tumours were stained with haematoxylin–eosin [42]. An Axiophot Zeiss photomicroscope with a SPOT digital camera was used.

Results

Preparation and characterization of the MJ7-Ngb immunotoxin

For the conjugation of MJ7/18 mAb to Ngb, we used SPDP since previous studies have shown this to be the best linker for Ngb in terms of the stability and anti-ribosomal activity of the derivatized toxin [39, 43, 44]. After the conjugation reaction, the molecular species were purified by chromatography on Superdex 200 HiLoad (26/60) and analysed by SDS-PAGE. As shown in Fig. 1a, the elution peak front accounted for slightly less than 50 % of the total protein used in the conjugation reaction. Only some fractions, which were pooled, met the requirements for selection as the immunotoxin. The apparent M_r values for small MJ7-Ngb immunotoxin material were between 206,000 and

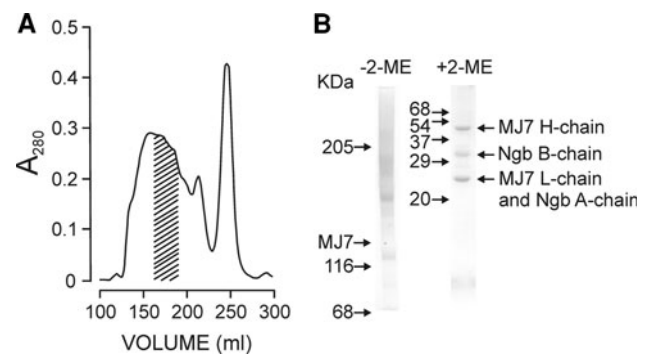


Fig. 1 Purification and SDS-PAGE analysis of the MJ7-Ngb immunotoxin. **a** The MJ7-Ngb immunotoxin was prepared by conjugation of Ngb and MJ7/18 mAb using the SPDP linker, as indicated in section “Materials and methods” and purified by gel filtration chromatography on Superdex 200 HiLoad. The *dashed area* indicates the fractions that were collected, pooled and subjected to SDS-PAGE. **b** Analysis of MJ7-Ngb immunotoxin by SDS-polyacrylamide gel electrophoresis in the absence or presence of 2-mercaptoethanol (2-ME) in 5 % (*left*) and 15 % (*right*) gels, respectively, and then stained with Coomassie blue. The *numbers* indicate the corresponding apparent M_r values of the standards (in kDa); *H* and *L* refer to the heavy and light chains of MJ7/18, respectively

318,000 (average apparent M_r assumed 262,000), thus indicating the presence of a mixture of conjugated species with an average stoichiometry that could be assumed to be 2 mol of Ngb per mol of MJ7/18 mAb (Fig. 1b). The preparation essentially lacked free antibody, as judged by SDS-PAGE. In the absence of 2-ME, the electrophoretic mobility revealed the presence of conjugates with M_r higher than 205,000, hereafter referred to as the MJ7-Ngb immunotoxin. The apparent polydispersity of the immunotoxins under non-reducing conditions is the consequence of the variability in protein–protein cross-links between Ngb and the monoclonal antibody. The cross-linking reagent SPDP reacts with lysine residues to form a stable amide bond linking both proteins through their lysine lateral chains. Because of the abundance of lysines in Ngb (14 residues) and antibody (about 80 residues), there are a large number of combinations and stoichiometries by which these two starting proteins can link together. By contrast, in the presence of 2-ME, the immunotoxin dissociated into its components bound by disulphide bridges, namely both the heavy (H) and light (L) chains of MJ7/18 and the A and B chains of Ngb; the L and A chains had a fairly similar M_r and therefore moved together. Chemical conjugation of proteins with biological activity usually affects, and most frequently reduces and even abolishes, their activities. Coupling of MJ7/18 mAb to Ngb did not alter the translational inhibitory activity of Ngb in the rabbit reticulocyte lysate model system at all (data not shown). This indicated that the Ngb molecules linked to MJ7/18 mAb had free access to its molecular target, that is, the rRNA loop in the large ribosomal subunit.

Cytotoxicity of MJ7-Ngb immunotoxin against the B16MEL4A5 and L929 cell lines

The expression of endoglin by the B16MEL4A5 and L929 mouse cell lines was studied by western blot using the MJ7/18 mAb, which is highly specific for mouse endoglin. As shown in Fig. 2a, the lysates of both cell lines expressed a reactive protein, namely the 180-kDa form in B16MEL4A5 cells and a slightly smaller form of 174 kDa in L929 cells. Although the presence of short and long

isoforms of endoglin has been described in human and murine tissues previously [41, 45], in our case, the size differences of endoglin were most probably due to the different degrees of glycosylation. An anti- β -actin antibody was used as a loading control.

We next assessed whether both forms of endoglin could be identified and targeted by the endoglin-specific immunotoxin. To assay the MJ7-Ngb immunotoxin on the B16MEL4A5 and L929 cell lines, we performed viability tests using the cell proliferation WST-1 reagent. As shown

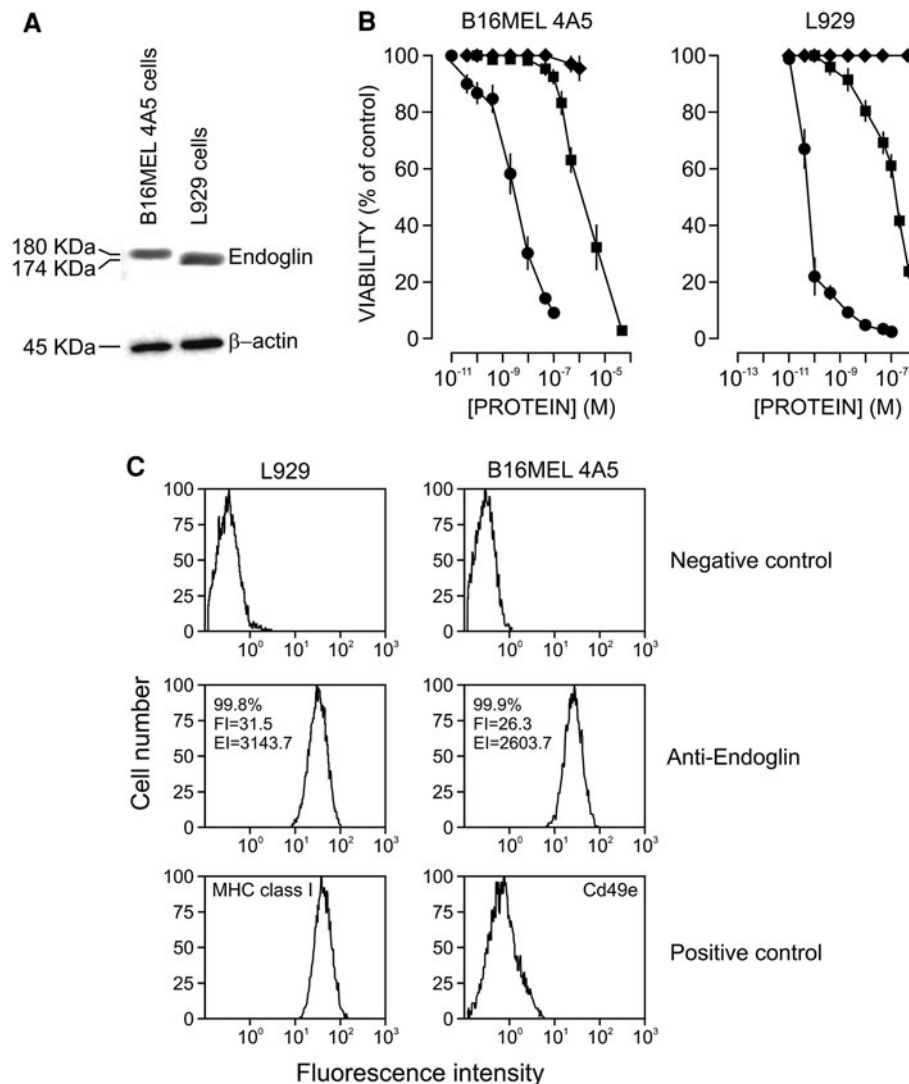


Fig. 2 Endoglin expression and cytotoxicity analyses. **a** Western blot analysis of endoglin and β -actin in total cell lysates from B16MEL4A5 and L929 mouse cell lines. Proteins were separated by SDS-PAGE under non-reducing conditions and specific bands were revealed using anti-endoglin (MJ7/18) and anti- β -actin (AC-15) mAbs. The apparent Mr values (in kDa) are indicated. **b** Cytotoxicity of MJ7-Ngb immunotoxin against B16MEL4A5 melanoma cells and L929 fibroblasts. Cells were incubated with increasing amounts of Ngb (squares), MJ7-Ngb immunotoxin (circles), unconjugated mAb (diamonds) for 3 h to permit internalization. Then, wells were washed

and cells were incubated with fresh complete medium for 72 h. The viability of the cells was assayed with the WST-1 reagent. Vertical bars indicate the SEM. **c** Flow cytometry analysis. B16MEL4A5 and L929 mouse cell lines were analysed by immunofluorescence flow cytometry with anti-endoglin (MJ7/18), anti-CD3 (Y-19) as negative control, anti-MHC class I (P2G9) as a positive control of L929 cells and anti-CD49e (5H10-27) as a positive control of melanoma cells. In anti-endoglin samples, the percentage of positive cells, the mean fluorescence intensity (FI) and the expression index (EI) are indicated

in Fig. 2b, the immunotoxin killed both cell lines but with different efficiencies. The IC_{50} values were 4.2×10^{-9} M for B16MEL4A5 and 7.7×10^{-11} M for L929 cells. As an internal control of toxicity, we assayed the effects of ricin on L929 cells and found an IC_{50} value very close to that obtained with the immunotoxin (data not shown) in agreement with data reported previously [38]. As expected, free Ngb was much less toxic than the immunotoxin, with IC_{50} values of 2.3×10^{-6} M for B16MEL4A5 and 2×10^{-7} M for L929 cells. The activity ratios between free Ngb and the immunotoxin were 0.55×10^3 and 0.26×10^4 for B16MEL4A5 and L929 cells, respectively. Of note, the MJ7/18 mAb alone was also inhibitory, although at concentrations much higher than those required to attain full inhibition by the immunotoxin (Fig. 2b). These results point to the high endoglin specificity of the immunotoxin.

In order to gain insights into the differences of sensitivity of both cell lines, an immunofluorescence flow cytometry assay on L929 and B16MEL4A5 cells using a rat mAb anti-mouse endoglin was carried out (Fig. 2c). Both cell types showed over 99.8 % of endoglin-positive cells with high mean fluorescence intensity, although the relative endoglin expression level of L929 cells was slightly higher than that of B16MEL4A5 cells (EI = 3143.7 in L929 vs EI = 2603.2 in B16MEL4A5 cells). In addition, the forward light scatter analysis indicated that the cell size of L929 was smaller than that of B16MEL4A5 cells with a size ratio L929/B16MEL4A5 of 0.87. Taken together, these data suggest that the relative surface density of endoglin is slightly higher in L929 than in B16MEL4A5 cells. Since the ratio L929/B16MEL4A5 of IC_{50} values is 0.018 (Fig. 2b), another factors should be taken into account. The effects of type 2 ribosome-inactivating proteins and immunotoxins on target cells are dependent, not only on the cell surface density of target antigens but also on their intracellular route which could modulate sensitive metabolic processes leading to different cell sensitivities. In this regard, melanoma cells are more resistant to free ricin and nigrin b than other cell lines, as previously reported [38].

Development of solid tumours in male C57BL/6 J mice

To study the *in vivo* effects of the immunotoxin, we promoted the development of solid tumours in C57BL/6 J male mice. To accomplish this, we injected variable amounts of B16MEL4A5 cells subcutaneously into the right flanks of the animals. As shown in Fig. 3, the tumours started to appear after approximately 8 days at the highest amount of cells injected (5×10^5 cells) rapidly reaching large sizes. At the lowest amount of cells injected (2×10^4 cells), palpable tumours started to appear in approximately half of the animals 20 days after cell injection. In the light

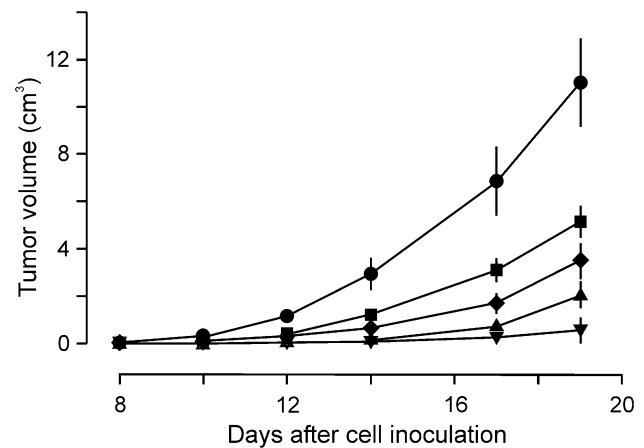


Fig. 3 Time course of the development of B16MEL4A5 melanoma tumours in mice, dependent on the number of cells injected. 2×10^4 (filled inverted triangle), 5×10^4 (filled triangle), 1.25×10^5 (filled diamond), 2.5×10^5 (filled square) and 5×10^5 (filled circle) B16MEL4A5 mouse melanoma cells were injected into the right flanks of C57BL/6 J mice. Tumour development and evolution were assessed by measuring their volume with a calliper

of these results, we selected the injection of 1.25×10^5 cells, which ensured fast and efficient development of tumours in all mice injected, but with a moderate increase in tumour size, in order to allow the immunotoxin to exert its potential effects.

In vivo activity of the MJ7-Ngb immunotoxin

Mice with palpable tumours 1–2 weeks after cell injection were assayed for immunotoxin treatment. We assayed different protocols that were found ineffective even though in some cases, at the same concentration tested herein but with 3 days of interval, the tumours started to become hard and somewhat bluish probably because the immunotoxin did not reach a minimal toxic plasma concentration. Pharmacokinetic studies on the murine anti-human endoglin mAb c-SN6j indicated that 24 and 48 h after its injection, the concentrations in plasma decreased 60 and 80 % respect to control (0 h), respectively [46]. Accordingly, we adjusted the intervals of our experiments to 12 h between injections, so under these conditions, the immunotoxin would be more effective. As shown in Fig. 4, control mice receiving no treatment, mice treated with MJ7/18 mAb and mice treated with free Ngb developed tumours of comparable size. In contrast, the treatment with immunotoxin exerted a significant inhibitory effect on tumour growth in comparison with the controls ($p < 0.05$). This inhibitory effect persisted up to 7 days, but after that time the tumours grew back. In most of the mice, tumour re-growth was slow. However, in some mice, the tumour started to grow very fast, reaching the size of the tumours of the control mice.

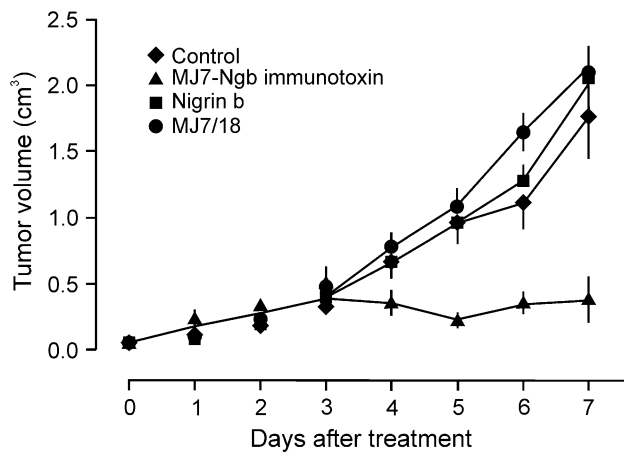


Fig. 4 Effects of the MJ7-Ngb immunotoxin on male C57BL/6 J mice bearing a palpable B16MEL4A5 mouse melanoma tumour. C57BL/6 J mice were injected with a suspension of 1.25×10^5 mouse B16MEL4A5 melanoma cells into the right flank, and tumour development and evolution were assessed by measuring their volume. The different treatments were initiated when the tumours became measurable

Figure 5 shows some typical tumour-bearing animals untreated and treated with the immunotoxin. The untreated animals exhibit a large solid tumour (Fig. 5a) with a well-defined shape as assessed by cross-sectional haematoxylin–eosin staining (Fig. 5e). The animals whose treatment led to apparently complete remission showed only fibrous material at the site formerly occupied by the tumour (Fig. 5b, c), and their cross-sectional view appears fibrous and almost devoid of proliferating cells (Fig. 5f, g). Figure 5d shows an animal with partial remission of a tumour; the cross-sectional view reveals a large number of live cells together with nearly a third of dead cells and fibrous tissue (Fig. 5h). In all cases where some kind of remission was observed, a large external injured area in the skin covering most of the original localization of the tumour was present, indicating derangement of the tumour mass.

In histological sections, the untreated tumours had large areas of densely arranged living tumour cells and smaller necrotic-haemorrhagic areas with a lower cell density (Fig. 6a). Melanin granules were unevenly distributed. The histological structure of the living cell areas showed a high degree of pleomorphism with a predominance of large cells with vesicular nuclei, multiple nucleoli and relatively abundant cytoplasm and mitoses (Fig. 6b). Among the tumour cells, there were numerous vascular spaces lacking a normal vascular wall, but instead lined by tumour cells (Fig. 6b). Some of the tumour cells adopted an endotheliiform disposition. The necrotic-haemorrhagic areas were formed by cells in different necrotic stages with pyknotic and karyorrhexic nuclei (Fig. 6c). In some places, the cellular debris and melanin granules were mixed with blood elements (Fig. 6c).

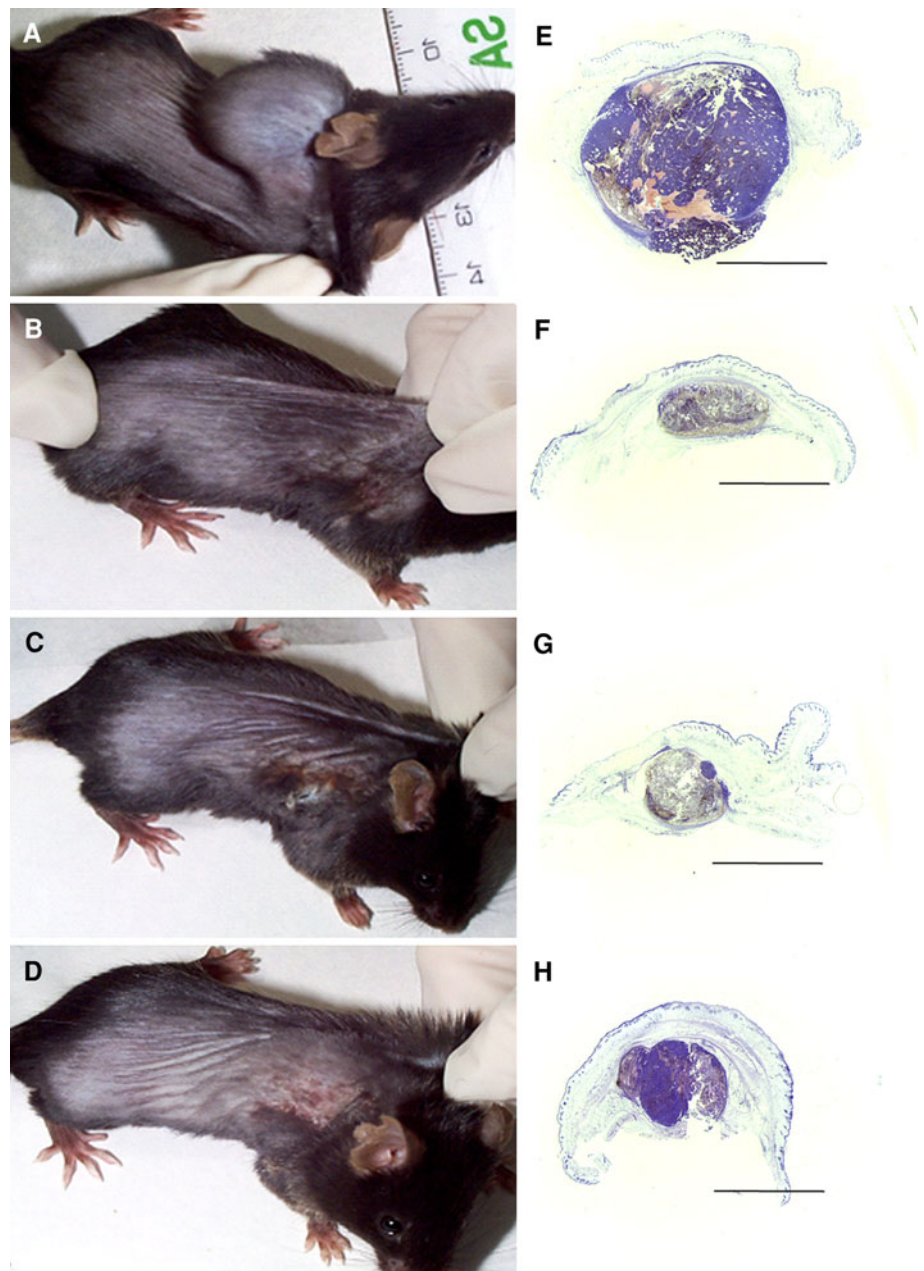
In the cases of almost complete tumour remission, a large fibrous area covering the previous location of the tumour was evident which means tumour mass derangement. The immunotoxin-treated tumours contained small living tumour cells areas and large necrotic-haemorrhagic areas (Fig. 6d). Melanin was also unevenly distributed and seemed to be more densely disposed than in the untreated tumours. The histological structure of the living tumour cell areas was similar to that of the untreated tumours. They were constituted by pleomorphic cells bearing large nuclei with irregularly condensed chromatin, and nucleoli were also evident (Fig. 6e). Mitoses were clearly less abundant in such tumour cell areas (0.77 in Fig. 5f and 2.26 in Fig. 5g) than in the corresponding ones of the untreated tumours (6.1 in Fig. 5e). The necrotic-haemorrhagic areas contained tumour cells with different degrees of necrosis including cells with homogeneously condensed nuclear chromatin and basophilic nuclear bodies (Fig. 6f). In these areas, melanin granules were more abundant than in living tumour cell areas.

Discussion

Mouse melanoma cells express endoglin, which can be detected with MJ7/18 mAb and can be targeted with an immunotoxin containing the same mAb linked to NgB through a disulphide bond. This immunotoxin was active against solid palpable B16MEL4A5 melanoma tumours developed in immunocompetent mice. As seen in the present study, the proof of concept of the effective anti-vascular action of an anti-endoglin immunotoxin works *in vivo*, most probably allowing simultaneous attack of the tumour by endoglin through two routes, namely freely accessible CD105+ B16MEL4A5 cells and the CD105+ endothelial cells of tumour neovessels. A sustained plasma concentration of immunotoxin above the minimal one required to trigger the effective attack against tumours, for instance by injection at proper intervals or by continuous intravenous infusion, could eliminate most of the new vessels and melanoma cells and thus hamper tumour development.

Ricin immunotoxins have proved to be useful in experimental therapy, and some clinical trials have been conducted to test their efficiency *in vivo* in patients with leukaemia and lymphoma [47, 48]. Perhaps, one of the main drawbacks of the use of ricin immunotoxins is the appearance of the so-called vascular leak syndrome [34]. In this sense, during our experiments with the NgB immunotoxin, we did not see patent evidence of general vascular leak syndrome or blood haemorrhages, except those concomitant with tumour derangement. Other complications could stem from the appearance of antibodies to mouse antibodies and ricin. Such problems could be circumvented to a

Fig. 5 External aspect of mice bearing a developed mouse melanoma untreated (**a**) or treated (**b–d**) for 7 days with the immunotoxin. Tumours were sectioned and stained with haematoxylin–eosin (**e–h**). In the immunotoxin-treated mice, the tumours were necrosed and a hardened and fibrous material accumulated in that area. **a, e** Tumours from untreated animals. **b, f** Apparent complete remission of tumours. **c, g** Large but incomplete remission of tumours. **d, h** Slight remission of tumours. Scale bar: 5 mm



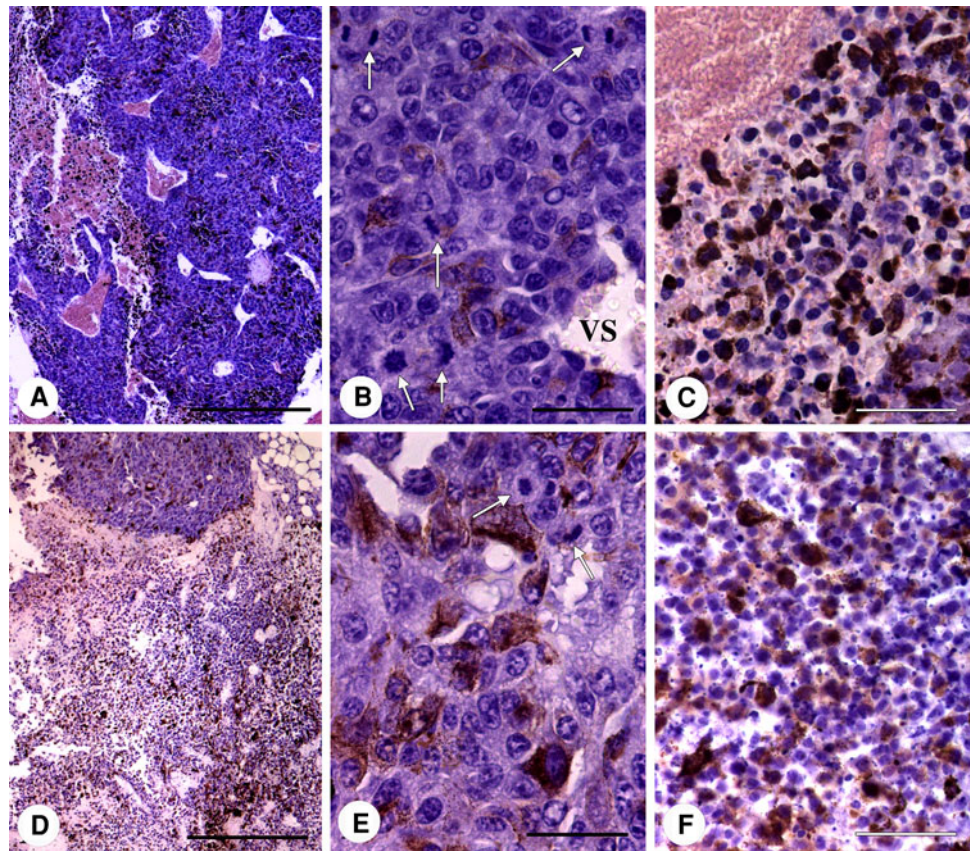
considerable extent by the use of humanized antibodies [49] and other toxic moieties, for instance Ngb, which is as active against ribosomes as ricin but lacks its non-specific toxicity [40, 50]. Of note, Ngb and other non-toxic type 2 ribosome-inactivating proteins from *Sambucus* were found to be poor immunogens and adjuvants when delivered intranasally to mice [51], in contrast to the highly toxic cholera toxin and mistletoe ribosome-inactivating proteins [52]. In any way, the possibility of limitations due to immunogenicity could be overcome by using immunosuppressors.

The differences in non-specific activity between Ngb and ricin have been discussed elsewhere [33]. They seem to

be related to subtle reductions in the affinity of Ngb for galactosides in comparison with ricin and also to the different pathways followed by both ribosome-inactivating proteins upon cell internalization [53]. Nonetheless, when coupled to the MJ7/18 mAb, Ngb follows the pathway taken up by the antibody, which results in its translocation to the cytosol and cell death.

As shown in this and previous work [39], Ngb forms an efficient immunotoxin with anti-CD105 monoclonal antibodies. The MJ7-bearing immunotoxin studied here efficiently targets endoglin, as reflected by its specific cytotoxicity in cultured mouse cells. These effects suggest

Fig. 6 Representative images of the untreated (a–c) and immunotoxin-treated melanomas (d–f). **a** An untreated tumour shows large living tumour cell areas and a few necrotic-haemorrhagic zones. **b** Living tumour cells with large vesicular nuclei, prominent nucleoli and a relatively dense cytoplasm. *White arrows*: mitoses. *VS*: vascular space surrounded by tumour cells. **c** Necrotic area with cells undergoing different degrees of destruction. **d** In immunotoxin-treated tumours, the living tumour cell areas are smaller than the predominant necrotic-haemorrhagic zones. **e** The living tumour cells of treated tumours are similar to those of the untreated tumours but with a lower degree of mitosis. **f** Necrotic-haemorrhagic zone of a treated tumour showing necrotic cells, melanin granules and basophilic bodies (*arrows*). *Scale bar* 500 μ m (a, d) or 50 μ m (b, c, e, f)



that endoglin is internalized and promotes the productive translocation of the immunotoxin to the cytosol, thus allowing the intracellular actions of Ngb. Ngb retains its anti-ribosomal toxicity after reaction with the MJ7/18 mAb and therefore exhibits cytotoxicity once targeted to CD105+ cells. It also retains its anti-ribosomal toxicity when coupled to ligands other than antibodies. We have previously constructed conjugates containing human transferrin and either Ngb or ebulin I both of which efficiently kill transferrin receptor-overexpressing HeLa cells [43]. Furthermore, conjugates made with Ngb and either SELld or SELfd, which are dimeric lectins, respectively, present in the leaves and fruits of dwarf elder (*Sambucus ebulus* L.) and which display a high affinity for mucins, have been constructed and were seen to exert strong cytotoxicity against human Colo 320 colon carcinoma cells [54]. In addition to its activity as a moiety of conjugates and immunotoxins, Ngb offers another important advantage from the pharmaceutical point of view derived from its very low toxicity *in vivo* and hence greater safety in its handling and manipulation as compared with ricin, abrin and other related toxic ribosome-inactivating proteins [33].

Our results indicate that the immunotoxin attacks vessels of rapidly growing melanoma tumours once created, when

the immunotoxin concentration is above the minimum required for cytotoxicity. This attack promotes the destruction of a sufficient number of endothelial cells to trigger blood haemorrhage in the growing tumour and further fibrosis in the same place. The exclusive derangement of the tumour area after the three consecutive injections reported here is clearly consistent with the increased expression of target endoglin, mainly in the tumour. In other words, the local increase in the density of both the long (melanoma cells) and short (vessels) forms of endoglin also increases the local targeting and cytotoxicity of the immunotoxin. This situation differs from that promoted by angiogenesis inhibitors, which merely inhibit the appearance of new blood vessels but do not destroy them once they have appeared, which does not seem to be sufficient for the complex therapy of cancer, as suggested recently [1].

In conclusion, cytotoxic vascular-targeting therapy with our immunotoxin could promote the destruction of newly created tumour vessels during the early stages of tumour development. Further work will address the effects of sustained administration of the immunotoxin for more prolonged treatments and its pharmacokinetic features in mice, the potential immunogenicity of the MJ7-Ngb construct and ways to prevent or circumvent it, if any.

Acknowledgments We thank J.E. Basterrechea for technical assistance and Dr. José M. Rojo (Centro de Investigaciones Biológicas, CSIC, Madrid) for providing us with anti-mouse antibodies. This research was supported by grants from the Junta de Castilla y León (Grupo de Excelencia GR106 and Convenio-Consejería de Sanidad) and UVA-GIR funding to T.G., Fondo de Investigaciones Sanitarias FISPI02/0917 to R.M. and FISPI04/1279 to J.M.F., *Ministerio de Ciencia e Innovación* of Spain (SAF2010-19222 to C.B.) and Genoma España (MEICA) to C.B. The *CIBER de Enfermedades Raras* is an initiative of the Instituto de Salud Carlos III (ISCIII).

Conflict of interest The authors report no conflict of interest.

References

- Roodink I, Leenders WP (2010) Targeted therapies of cancer: angiogenesis inhibition seems not enough. *Cancer Lett* 299(1):1–10. doi:10.1016/j.canlet.2010.09.004
- Fukumura D, Jain RK (2007) Tumor microenvironment abnormalities: causes, consequences, and strategies to normalize. *J Cell Biochem* 101(4):937–949. doi:10.1002/jcb.21187
- Carmeliet P, Jain RK (2011) Molecular mechanisms and clinical applications of angiogenesis. *Nature* 473(7347):298–307. doi:10.1038/nature10144
- Boehm T, Folkman J, Browder T, O'Reilly MS (1997) Antiangiogenic therapy of experimental cancer does not induce acquired drug resistance. *Nature* 390(6658):404–407. doi:10.1038/37126
- Kerbrel RS, Folkman J (2002) Clinical translation of angiogenesis inhibitors. *Nat Rev Cancer* 2(10):727–739. doi:10.1038/nrc905
- Mitchell DC, Bryan BA (2010) Anti-angiogenic therapy: adapting strategies to overcome resistant tumors. *J Cell Biochem* 111(3):543–553. doi:10.1002/jcb.22764
- Gasparini G, Longo R, Fanelli M, Teicher BA (2005) Combination of antiangiogenic therapy with other anticancer therapies: results, challenges, and open questions. *J Clin Oncol* 23(6):1295–1311. doi:10.1200/JCO.2005.10.022
- Seon BK, Matsuno F, Haruta Y, Kondo M, Barcos M (1997) Long-lasting complete inhibition of human solid tumors in SCID mice by targeting endothelial cells of tumor vasculature with antihuman endoglin immunotoxin. *Clin Cancer Res* 3(7):1031–1044
- Thorpe PE (2004) Vascular targeting agents as cancer therapeutics. *Clin Cancer Res* 10(2):415–427. doi:10.1158/1078-0432.CCR-0642-03
- Gerber H-P, Senter PD, Grewal IS (2009) Antibody drug-conjugates targeting the tumor vasculature: current and future developments. *MAbs* 1(3):247–253. doi:10.4161/mabs.1.3.8515
- Madlambayan GJ, Meacham AM, Mir KS, Jorgensen M, Scott EW, Siemann DW, Cogle CR (2010) Leukemia regression by vascular disruption and antiangiogenic therapy. *Blood* 116(9):1539–1547. doi:10.1182/blood-2009-06-230474
- Clément-Duchêne C, Wakelee H (2010) Antiangiogenic agents and vascular disrupting agents for the treatment of lung cancer: a review. *J Thorac Oncol* 5(1):129–139. doi:10.1097/JTO.0b013e3181c59a60
- Escorcía FE, Henke E, McDevitt MR, Villa CH, Smith-Jones P, Blasberg RG, Benezra R, Scheinberg DA (2010) Selective killing of tumor neovasculature paradoxically improves chemotherapy delivery to tumors. *Cancer Res* 70(22):9277–9286. doi:10.1158/0008-5472.CAN-10-2029
- Ulinisky T, Lervat C, Ranchin B, Gillet Y, Floret D, Cochat P (2005) Neonatal haemolytic uremic syndrome after mother-to-child transmission of *Escherichia coli* O157. *Pediatr Nephrol* 20(9):1334–1335. doi:10.1007/s00467-005-1871-3
- Fonsatti E, Sigalotti L, Arslan P, Altomonte M, Maio M (2003) Emerging role of endoglin (CD105) as a marker of angiogenesis with clinical potential in human malignancies. *Curr Cancer Drug Targets* 3(6):427–432
- Jerkic M, Rodríguez-Barbero A, Prieto M, Toporsian M, Pericacho M, Rivas-Elena JV, Obreo J, Wang A, Pérez-Barriocanal F, Arévalo M, Bernabéu C, Letarte M, López-Novoa JM (2006) Reduced angiogenic responses in adult endoglin heterozygous mice. *Cardiovasc Res* 69(4):845–854. doi:10.1016/j.cardiores.2005.11.020
- López-Novoa JM, Bernabéu C (2010) The physiological role of endoglin in the cardiovascular system. *Am J Physiol Heart Circ Physiol* 299(4):H959–H974. doi:10.1152/ajpheart.01251.2009
- Düwel A, Eleno N, Jerkic M, Arevalo M, Bolaños JP, Bernabéu C, López-Novoa JM (2007) Reduced tumor growth and angiogenesis in endoglin-haploinsufficient mice. *Tumour Biol* 28(1):1–8
- Bernabéu C, Lopez-Novoa JM, Quintanilla M (2009) The emerging role of TGF-beta superfamily coreceptors in cancer. *Biochim Biophys Acta* 1792(10):954–973. doi:10.1016/j.bbdis.2009.07.003
- Fonsatti E, Nicolay HJ, Altomonte M, Covre A, Maio M (2010) Targeting cancer vasculature via endoglin/CD105: a novel antibody-based diagnostic and therapeutic strategy in solid tumors. *Cardiovasc Res* 86(1):12–19. doi:10.1093/cvr/cvp332
- Hussein MR (2005) Transforming growth factor-beta and malignant melanoma: molecular mechanisms. *J Cutan Pathol* 32(6):389–395. doi:10.1111/j.0303-6987.2005.00356.x
- Sun T, Sun BC, Ni CS, Zhao XL, Wang XH, Qie S, Zhang DF, Gu Q, Qi H, Zhao N (2008) Pilot study on the interaction between B16 melanoma cell-line and bone-marrow derived mesenchymal stem cells. *Cancer Lett* 263(1):35–43. doi:10.1016/j.canlet.2007.12.015
- Letamendia A, Lastres P, Almendro N, Raab U, Bühring HJ, Kumar S, Bernabéu C (1998) Endoglin, a component of the TGF-beta receptor system, is a differentiation marker of human choriocarcinoma cells. *Int J Cancer* 76(4):541–546. doi:10.1002/(SICI)1097-0215(19980518)
- Kumar S, Ghellal A, Li C, Byrne G, Haboubi N, Wang JM, Bundred N (1999) Breast carcinoma: vascular density determined using CD105 antibody correlates with tumor prognosis. *Cancer Res* 59(4):856–861
- Romani AA, Borghetti AF, Del Rio P, Sianesi M, Soliani P (2006) The risk of developing metastatic disease in colorectal cancer is related to CD105-positive vessel count. *J Surg Oncol* 93(6):446–455. doi:10.1002/jso.20456
- Marioni G, D'Alessandro E, Giacomelli L, Staffieri A (2010) CD105 is a marker of tumour vasculature and a potential target for the treatment of head and neck squamous cell carcinoma. *J Oral Pathol Med* 39(5):361–367. doi:10.1111/j.1600-0714.2010.00888.x
- Li C, Guo B, Wilson PB, Stewart A, Byrne G, Bundred N, Kumar S (2000) Plasma levels of soluble CD105 correlate with metastasis in patients with breast cancer. *Int J Cancer* 89(2):122–126. doi:10.1002/(SICI)1097-0215(20000320)89:2<122::AID-IJC4>3.0.CO;2-M
- Dallas NA, Samuel S, Xia L, Fan F, Gray MJ, Lim SJ, Ellis LM (2008) Endoglin (CD105): a marker of tumor vasculature and potential target for therapy. *Clin Cancer Res* 14(7):1931–1937. doi:10.1158/1078-0432.CCR-07-4478
- Uneda S, Toi H, Tsujie T, Tsujie M, Harada N, Tsai H, Seon BK (2009) Anti-endoglin monoclonal antibodies are effective for suppressing metastasis and the primary tumors by targeting tumor vasculature. *Int J Cancer* 125(6):1446–1453. doi:10.1002/ijc.24482
- Seon BK, Haba A, Matsuno F, Takahashi N, Tsujie M, She X, Harada N, Uneda S, Tsujie T, Toi H, Tsai H, Haruta Y (2011) Endoglin-targeted cancer therapy. *Curr Drug Deliv* 8(1):135–143

31. Pastan I, Hassan R, Fitzgerald DJ, Kreitman RJ (2006) Immunotoxin therapy of cancer. *Nat Rev Cancer* 6(7):559–565. doi:[10.1038/nrc1891](https://doi.org/10.1038/nrc1891)
32. Olsnes S, Kozlov JV (2001) Ricin. *Toxicol* 39(11):1723–1728. doi:[10.1016/S0041-0101\(01\)00158-1](https://doi.org/10.1016/S0041-0101(01)00158-1)
33. Girbes T, Ferreras JM, Arias FJ, Stirpe F (2004) Description, distribution, activity and phylogenetic relationship of ribosome-inactivating proteins in plants, fungi and bacteria. *Mini Rev Med Chem* 4(5):461–476
34. Baluna R, Vitetta ES (1997) Vascular leak syndrome: a side effect of immunotherapy. *Immunopharm* 37(2–3):117–132. doi:[10.1016/S0162-3109\(97\)00041-6](https://doi.org/10.1016/S0162-3109(97)00041-6)
35. Basu B, Biswas S, Wrigley J, Sirohi B, Corrie P (2009) Angiogenesis in cutaneous malignant melanoma and potential therapeutic strategies. *Expert Rev Anticancer Ther* 9(11):1583–1598. doi:[10.1586/era.09.135](https://doi.org/10.1586/era.09.135)
36. Thompson JF, Scolyer RA, Kefford RF (2005) Cutaneous melanoma. *Lancet* 365(9460):687–701. doi:[10.1016/S0140-6736\(05\)17951-3](https://doi.org/10.1016/S0140-6736(05)17951-3)
37. Schmidt P, Abken H (2011) The beating heart of melanomas: a minor subset of cancer cells sustains tumor growth. *Oncotarget* 2(4):313–320
38. Muñoz R, Arias Y, Ferreras JM, Jiménez P, Rojo MA, Girbés T (2001) Sensitivity of cancer cell lines to the novel non-toxic type 2 ribosome-inactivating protein nigrin b. *Cancer Lett* 167(2):163–169. doi:[10.1016/S0304-3835\(01\)00477-3](https://doi.org/10.1016/S0304-3835(01)00477-3)
39. Muñoz R, Arias Y, Ferreras JM, Rojo MA, Gayoso MJ, Nocito M, Benítez J, Jiménez P, Bernabéu C, Girbés T (2007) Targeting a marker of the tumour neovasculature using a novel anti-human CD105-immunotoxin containing the non-toxic type 2 ribosome-inactivating protein nigrin b. *Cancer Lett* 256(1):73–80. doi:[10.1016/j.canlet.2007.05.012](https://doi.org/10.1016/j.canlet.2007.05.012)
40. Girbés T, Citores L, Ferreras JM, Rojo MA, Iglesias R, Muñoz R, Arias FJ, Calonge M, García JR, Méndez E (1993) Isolation and partial characterization of nigrin b, a non-toxic novel type 2 ribosome-inactivating protein from the bark of *Sambucus nigra* L. *Plant Mol Biol* 22(6):1181–1186
41. Raab U, Velasco B, Lastres P, Letamendía A, Calés C, Langa C, Tapia E, López-Bote JP, Páez E, Bernabéu C (1999) Expression of normal and truncated forms of human endoglin. *Biochem J* 339:579–588
42. Gayoso MJ, Muñoz R, Arias Y, Villar R, Rojo MA, Jiménez P, Ferreras JM, Aranquez I, Girbés T (2005) Specific dose-dependent damage of Lieberkühn crypts promoted by large doses of type 2 ribosome-inactivating protein nigrin b intravenous injection to mice. *Toxicol Appl Pharmacol* 207(2):138–146. doi:[10.1016/j.taap.2004.12.011](https://doi.org/10.1016/j.taap.2004.12.011)
43. Citores L, Ferreras JM, Muñoz R, Benítez J, Jiménez P, Girbés T (2002) Targeting cancer cells with transferrin conjugates containing the non-toxic type 2 ribosome-inactivating proteins nigrin b or ebulin I. *Cancer Lett* 184(1):29–35. doi:[10.1016/S0304-3835\(02\)00169-6](https://doi.org/10.1016/S0304-3835(02)00169-6)
44. Benítez J, Ferreras JM, Muñoz R, Arias Y, Iglesias R, Córdoba-Díaz M, Del Villar R, Girbés T (2005) Cytotoxicity of an Ebulin I-anti-human CD105 Immunotoxin on mouse fibroblasts (L929) and rat myoblasts (L6E9) cells expressing human CD105. *Med Chem* 1(1):65–70
45. Pérez-Gómez E, Eleno N, López-Novoa JM, Ramirez JR, Velasco B, Letarte M, Bernabéu C, Quintanilla M (2005) Characterization of murine S-endoglin isoform and its effects on tumor development. *Oncogene* 24(27):4450–4461. doi:[10.1038/sj.onc.1208644](https://doi.org/10.1038/sj.onc.1208644)
46. Shiozaki K, Harada N, Greco WR, Haba A, Uneda S, Tsai H, Seon BK (2006) Antiangiogenic chimeric antiendoglin (CD105) antibody: pharmacokinetics and immunogenicity in nonhuman primates and effects of doxorubicin. *Cancer Immunol Immunother* 55(2):140–150. doi:[10.1007/s00262-005-0691-4](https://doi.org/10.1007/s00262-005-0691-4)
47. Dinndorf P, Krailo M, Liu-Mares W, Friedrich S, Sondel P, Reaman G (2001) Phase I trial of anti-B4-blocked ricin in pediatric patients with leukemia and lymphoma. *J Immunother* 24(6):511–516
48. Herrera L, Bostrom B, Gore L, Sandler E, Lew G, Schlegel PG, Aquino V, Ghetie V, Vitetta ES, Schindler J (2009) A phase I study of Combotox in pediatric patients with refractory B-lineage acute lymphoblastic leukemia. *J Pediatr Hematol Oncol* 31(12):936–941. doi:[10.1097/MPH.0b013e3181bdf211](https://doi.org/10.1097/MPH.0b013e3181bdf211)
49. Weiner LM (2006) Fully human therapeutic monoclonal antibodies. *J Immunother* 29(1):1–9
50. Battelli MG, Citores L, Buonamici L, Ferreras JM, De Benito FM, Stirpe F, Girbés T (1997) Toxicity and cytotoxicity of nigrin b, a two-chain ribosome-inactivating protein from *Sambucus nigra*: a comparison with ricin. *Arch Toxicol* 71(6):360–364
51. Lavelle EC, Grant G, Pfüller U, Girbés T, Jiménez P, Pusztai A, Leavy O, Mills KH, O'Hagan DT (2000) Mistletoe lectins are strong mucosal adjuvants. *Immunol* 101:32
52. Lavelle EC, Grant G, Pusztai A, Pfüller U, Leavy O, MacNeela E, Mills KH, O'Hagan DT (2002) Mistletoe lectins enhance immune responses to intranasally co-administered herpes simplex virus glycoprotein D2. *Immunology* 107(2):268–274. doi:[10.1046/j.1365-2567.2002.01492.x](https://doi.org/10.1046/j.1365-2567.2002.01492.x)
53. Ferreras JM, Citores L, Iglesias R, Jiménez P, Girbés T (2010) *Sambucus* ribosome-inactivating proteins and lectins. *Toxic plant proteins. Plant Cell Monogr* 18:107–131. doi:[10.1007/978-3-642-12176-0_6](https://doi.org/10.1007/978-3-642-12176-0_6)
54. Benítez J, Rojo MA, Muñoz R, Ferreras JM, Jiménez P, Girbés T (2004) Design and cytotoxicity analysis of a conjugate containing the new D-galactose-binding lectin SELId and the non-toxic type 2 ribosome inactivating protein nigrin b. *Lett Drug Des Discov* 1:361–367